Seabed characterization by a thin-line towed array using acoustic communication signals

Nicholas P. Chotiros
Applied Research Laboratories
The University of Texas at Austin
Texas, USA
chotiros@arlut.utexas.edu

Venugopalan Pallayil
Acoustic Research Laboratory
Tropical Marine Science Institute
National University of Singapore
119223, Singapore
venu@arl.nus.edu.sg

***Abstract*— Bottom reflection loss, measured on an autonomous underwater vehicle with a small thin-line towed array, was used to estimate bottom sediment type. The self-noise of the AUV was used as the signal source. The critical issue was identifying the direct path and bottom reflected components of the signal. The method is robust because it does not require absolute calibrations. The ratio of the direct and bottom bounce signals, after accounting for differences in spreading loss, is used to estimate the bottom loss and its phase, which may be compared to suitable models to obtain an estimate of bottom type. Results obtained over a soft sediment indicate acoustic impedances both greater and less than that of water.**

Keywords— marine sediment; reflection loss; underwater acoustics; towed array

I. Introduction

The inversion of environmental properties using a known source and an array of receivers towed by a research vessel is a standard procedure [1][2][3]. The source and receiver may be towed at any desired depth for optimal performance. With the advent of autonomous underwater vehicles (AUVs) and thin-line towed arrays, the hardware may be significantly reduced in size, and the towing ship no longer required [4][5][6]. The concept is illustrated in Fig. 1.

The signal is projected from the AUV and reflected by the surface and bottom. Only the single bounce paths are shown, although in reality there are numerous multipaths. To measure the bottom reflection coefficient, it is only necessary to separate the direct path signal from the bottom reflected signal. Using the known distance from source to receiver, the path length of the bottom reflected signal, and the beam patterns of the source and receiver, the differences in spreading and absorption losses and directivity functions may be accounted for. After removing the differences in the losses and directivity functions, the amplitude of the bottom reflection coefficient is simply the ratio of the bottom reflected signal amplitude to the direct path signal amplitude. The method is simple and robust because it does not require any absolute calibrations of the sources and receivers. This paper is a discussion of a recent study by the authors that will appear in the IEEE Journal of Oceanic Engineering [7]. Both amplitude and phase of the bottom reflection coefficient are accessible.

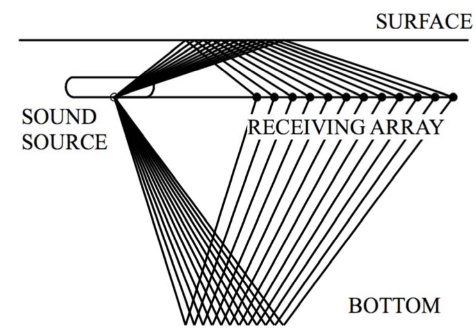

Fig. 1. Concept of an AUV and towed line array, with a sound source on the AUV and surface and bottom bounced sound rays between source and the receiver array.

II. Sound source

Without a dedicated sound source, it is possible to use a source of opportunity. A source on the vehicle itself is preferred in order to provide relatively small, known angles of incidence on the bottom. The noise from the propulsion system was a possible candidate, but in this case it was too faint to be detected. The acoustic communications (AC) signal projector turned out to be the most prominent source of noise. Since the AC signal is not a well-defined discrete pulse, it is necessary to synthesize the equivalent pulses using the auto-correlation function of the received signal. The received signals were further complicated by the presence of electrical interference from the acoustic communication signal generator. Another complication was that the signal was under-sampled which puts the AC signal into an aliased part of the spectrum. As a result, the auto-correlation diagrams were considerably more complicated than what one would expect from the simple concept diagram in Fig. 1.

Work supported by the U.S. Office of Naval Research, Ocean Acoustics Program.

978-0-933957-40-4 ©2013 MTS

III. EXPERIMENT

The experiment was conducted near the NATO Undersea Research Centre (NURC) at San Bartolomeo 400, La Spezia, Italy. While the main objective was to evaluate the performance of the Digital Thin Line Array (DTLA) [8],[9], seabed type characterization was added at the post processing stage. The experiments were performed from 19th to 23rd June 2009. The tow platform used was the Ocean Explorer (OEX), an AUV provided by NURC. The DTLA was developed by the Acoustics Research Laboratory, National University of Singapore. It was 10.5 mm in diameter and about 20 m long with its tow cable included. The data used for this study were from recordings collected on 23rd June. The AUV was making rectangular loops of sides 250 and 50 m and the total data collection was for 40 minutes over four such loops. The speed of tow during these experiments varied from 1.4 to 2.8 knots. The experiment took place in the inner part (within the breakwater) of the Gulf of La Spezia, near the NURC. The sea surface was calm.

The data collected were divided in time into 40-second contiguous blocks for correlation processing. Given the signal bandwidth of approximately 10 kHz, a 40 second block could contain up to 400,000 independent samples, which should be adequate for constructing statistically meaningful correlation functions. Since the signals were communication signals that changed with the content of the message, they could only be treated statistically. The direct and bottom bounce signals had to be extracted from the auto- and cross correlation functions.

The data processing was complicated by the presence of an electrical feed-over of the AC signal into all receiver channels. When contaminated by the electrical feed-over, the autocorrelation function of signal at each hydrophone produced a peak at the a delay equal to the direct path travel time through the water between the AC source and the hydrophone. Making a virtue of necessity, this peak was used to esimate the trail-back of the array. A plot of the trail-back of the closest hydrophone, as shown in Fig. 2, is an indicator of the stability of the towed array. In the first 400 seconds, the array was unstable because a stable correlation peak could not be found. Between 400 and 600 seconds, a correlation peak was detectable and the trail-back was found to fluctuate about 5.9 m. After 600 seconds, the trail-back settled down to a value of approximately 6.0 meters, which was the design value. There were gaps in the trail back estimates at more-or-less regular intervals in which the correlation peak was unstable. These were likely caused by the vehicle executing tight turns at the ends of the straight tracks along the long sides of the rectangular path. Only the data sections in which the trail-back was stable were used for subsequent analysis.

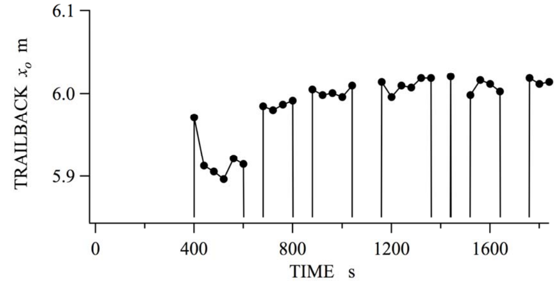

Fig. 2. Measured trail-back distance, from AC source to the nearest receiver, as a function of time in each data block.

An example of the autocorrelation function magnitudes is shown in Fig. 3. There are a number of ridges that appear to cross one another in a rather confusing manner. A detailed explanation is available in [7]. An example from the sea test data is shown in the top panel (a) while a simulation is shown in the bottom panel (b) for comparison. The expected positions of the ridges due to the cross-correlation between the direct path signal and the surface and bottom reflected signals (DIR_SURF, DIR_BOT) are visible in the simulation but difficult to find in the data. The ridges that dominate are the ones associated with the electrical feed-over signal, including the cross correlation between the feed-over and the direct path signal (FO_DIR), and the bottom bounce signal (FO_BOT). There are periodic repetitions of certain ridges (FO_DIR+REP) due to the modulation of the signal spectrum envelope, which causes time side-lobes. The FO_DIR ridge was used to estimate trail-back since it gives the acoustic travel time from source to the array element. It clearly shows the travel time from source to each array element. The signal from the nearest element is labeled "Channel 1" and so on.

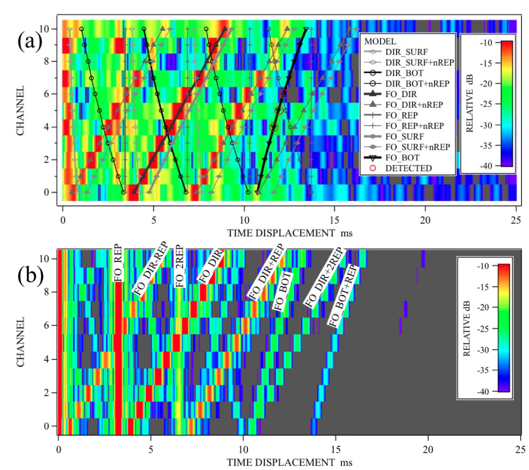

Fig. 3. (a) Example of the measured autocorrelation functions, and the expected ridges. (b) Example of simulated autocorrelation functions, showing periodically repeating ridges FO_REP, FO_DIR_-REP, and FO_DIR+REP.

IV. Estimation of Bottom Loss

A. Ratio of bottom bounce path to direct path signals

In the absence of calibration, the reflection coefficient $R_i(\theta)$, as a function of the grazing angle θ, may be defined in terms of the ratio between the direct path signal S_{iD} and the bottom reflected signal S_{iR}, at array element number i, after compensating for differences in spreading loss, absorption and directivity functions.

$$R_i(\theta) = \frac{S_{iR} D_{iD} r_{iR} \exp(\alpha r_{iR})}{S_{iD} D_{iR} r_{iD} \exp(\alpha r_{iD})} \tag{1}$$

The quantites r_{iD} and r_{iR} are the path lengths, and D_{iD} and D_{iR} are directivity functions, from source to receiver along the direct and reflected paths, respectively, and θ is the absorption coefficient. It is assumed that the sound speed in the water may be approximated by a constant. This is a valid assumption, because the path lengths are very short, and because the sound speed profile at the site was known to be benign. The absorption may be ignored because it is estimated to be less than 0.004 dB/m, and the path lengths are less than 20 meters, giving absorption losses of less than 0.1 dB. The AC source directivity may be considered approximately uniform in the horizontal and downward directions.

The beampattern of the source may be considered omnidirectional for practical purposes. The directivity function of the array elements, in the applicable frequency band, is needed to be taken into consideration. Each array element consisted of a small horizontal array of 6 serially connected sensors, with their centers spaced at 10.5 mm apart. Based on this physical arrangement, the average directivity function of the element, for the applicable frequency band was computed. A reduction of 7.8 dB in the horizontal (direct path) direction relative to the bottom reflected direction was predicted.

B. Autocorrelation functions

The original plan was to estimate the ratio between the direct path signal S_{iD} and the bottom reflected signal S_{iR} from their cross correlation ridge (DIR_BOT) and the peak at t=0, but it was obscured by the stronger ridges associated with the feed-over (FO_DIR, and FO_DIR+/-REP). Instead, this ratio was obtained from the ratio of the autocorrelation amplitude at FO_BOT to that at the FO_DIR positions. The former is the cross-correlation between the feed-over and the bottom reflected signal, and the latter the cross-correlation between the feed-over and the direct path signal. One contains a product of the feed-over and bottom reflected signal, and the other the product of the feed-over and the direct path signal. Dividing one by the other eliminates the feed-over, leaving the ratio of the reflected and direct path signals. Both amplitude and phase are available, as shown in Eqs. (2) and (3).

$$\left| \frac{S_{iR}}{S_{iD}} \right| = \left| \frac{C_i(t_{i,FO\_BOT})}{C_i(t_{i,FO\_DIR})} \right| \tag{2}$$

$$\arg\left(\frac{S_{iR}}{S_{iD}} \right) = \arg\left(\frac{C_i(t_{i,FO\_BOT})}{C_i(t_{i,FO\_DIR})} \right) \tag{3}$$

The term $C_i(t)$ is the autocorrelation function of the ith array element at time t, and the times t_{i,FO_BOT} and t_{i,FO_DIR} are the delay times of the respective correlation peaks, of the feed-over signal to the bottom bounce signal, and of the feed-over signal to the direct path signal.

The amplitude ratio may be substituted into Eq. (1) to estimate the magnitude of the bottom reflection loss. Although the directivity functions D_{iD} and D_{iR} in Eq. (1) may be complex, mostly their magnitude are likely to vary with direction, and therefore their ratios would be approximately real. In that case, the phase of the reflection coefficient would be approximately equal to the phase given by Eq. (3).

Finally, with reference to Fig. 1, the grazing angle θ may be related to the travel time difference (t_{i,FO_BOT} - t_{i,FO_DIR}), the speed of sound in water c, and the height above the seabed (d_b-d_s),

$$\tan(\theta) = \frac{2(d_b - d_s)}{(t_{i,FO\_BOT} - t_{i,FO\_DIR})c} \tag{4}$$

C. Results

Using the above method, the bottom reflection loss estimates were made. A histogram of the measured values, in 5 dB bins, is shown in Fig. 4. There is a single peak centered around -21 dB with a standard deviation of 4.9 dB, indicating a soft sediment. This is consistent with previous surveys of the area [10]. The grazing angles were centered on a mean of 62 degrees, with a standard deviation of 5 degrees. A scatter plot of reflection loss a function of phase, as calculated by Eq. (3) is shown in Fig. 5. The data appears to be divisible by phase into two groups. The first group has 102 samples, a mean of -.98 and a standard deviation of .8 radians; the other has 68 samples, a mean of 2.18 and a standard deviation of 0.4 radians. It is observed that the mean values differ by almost exactly π radians. These results suggest that the first group, which contains the majority of the data points, is what one would usually expect from a bottom with a higher acoustic impedance than the water. The mean phase shift of -.98 radians is likely an average phase bias caused by the directivity functions of source and receivers. The second group, which has a relative phase shift of π radians, must be due to very soft or even bubbly patches, in which the acoustic impedance is lower than that of the water.

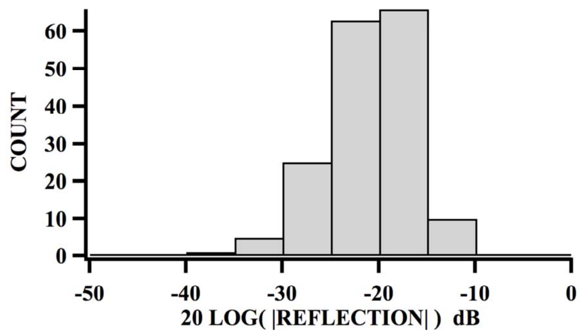

Fig. 4. Histogram of measured reflection loss.

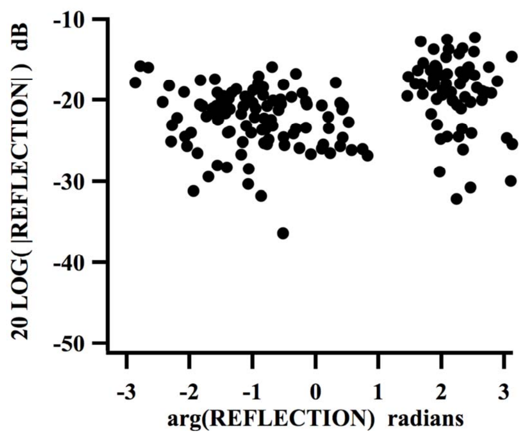

Fig. 5. Reflection amplitude as a function of phase.

ACKNOWLEDGMENT

The authors wish to thank their colleagues, particularly Mandar Chitre and Marcia Isakson, for many useful discussions, and to acknowledge the NURC for the support in providing the OEX platform for the data collection.

REFERENCES

[1] N. H. Gholson and M. G. Fagot, "A Deep-Towed Sound Source and Hydrophone Array System-Performance Analysis and Design," in Handbook of Geophysical Exploration at Sea, R. A. Geyer, Ed. Boca Raton, FL, USA: CRC Press, Inc., 1983.

[2] J. F. Gettrust, J. H. Ross, and M. M. Rowe, "Development of a low frequency, deep tow geoacoustic system," Sea Technology, vol. September, 1991, pp. 23-32.

[3] C. W. Holland and J. Osler, "High-resolution geoacoustic inversion in shallow water: A joint time- and frequency-domain technique," J. Acoust. Soc. Am. 107(3), pp. 1263-1280, 2000.

[4] J. D. Holmes, W. M. Carey, and J. F. Lynch, "Results from an autonomous underwater vehicle towed hydrophone array experiment in Nantucket Sound," J. Acoust. Soc. Am. EL, vol. 120, pp. EL15-EL21, 2006.

[5] A. Maguer, R. Dymond, P. Guerrini, L. Troiano, V. Grandi, A. Figoli, C. Olivero, A. Sapienza, S. Fioravanti, and J. Potter, "Receiving and transmitting acoustic systems for AUV/gliders," in Underwater Acoustic Measurements: Technologies and Results, 3rd International Conference, Nafplion, Greece, 2009.

[6] C. W. Holland, P. L. Nielsen, J. Dettmer, and S. E. Dosso, "Resolving meso-scale seabed variability using reflection measurements from an autonomous underwater vehicle," J. Acoust. Soc. Am., vol. 131, pp. 1066-1078, 2012.

[7] N. P. Chotiros and V. Pallayil, “Seabed characterisation using acoustic communication signals on an autonomous underwater vehicle with a thin-line towed array,” IEEE J. Ocean Eng. (accepted for publication in a future issue, 2013).

[8] V. Pallayil, M. A. Chitre, and P. D. Deshpande, "A Digital Thin Line Towed Array for Small Autonomous Underwater Platforms," in Proceedings of the Oceans 2007 MTS/IEEE Vancouver Conference and Exhibition, Vancouver, BC, Canada, 29 September - 4 October 2007.

[9] V. Pallayil, S. S. Muttuthupara, M. A. Chitre, K. Govind V, and N. R. Chandhavarkar, "Characterisation of a digital thin line towed array – experimental assessment of vibration levels and tow shape," Underwater Acoustic Measurements: Technologies and Results, 3rd International Conference, Nafplion, Greece, 21-26 June 2009.

[10] L. R. Breslau and H. E. Edgerton, "The sub-bottom structure of the gulf of La Spezia," SACLANT ASW Research Centre, La Spezia, Italy, Technical Report No. 129, 1 December 1968, Available: http://www.dtic.mil/dtic/tr/fulltext/u2/845867.pd